mathematics

MDPI

Article

Research on the Calculation Method of Electrostatic Field of a Thunderstorm Cloud

Lin Wang, Haojiang Wan and Yazhou Chen *

Key Laboratory on Electromagnetic Environmental Effects, Shijiazhuang Campus, Army Engineering University, Shijiazhuang 050003, China

* Correspondence: chen_yazhou@sina.com

Abstract: The electrostatic field in the space excited by a thunderstorm cloud reflects the trend of the spatial potential and has a great influence on the selection of lightning discharge paths. Some studies have used an approximate method to calculate the electrostatic field excited by a thunderstorm cloud, but the error is still relatively large. In order to improve the computational accuracy, the second-order approximate solution of the electric field is obtained in this paper by using a binomial expansion of the complex quantized function, discarding the higher-order small terms and integrating the main term according to the convergence of the function. The first-order approximate solution and the second-order approximate solution are used to calculate the electrostatic field excited by a thunderstorm cloud using the same version of MATLAB on the same configuration of computers. By comparison, it is found that the computation time using the two approximate solutions is not much different, but the error between the second-order approximate solution and the exact solution is significantly smaller than that between the first-order approximate solution and the exact solution. It is shown that using the second-order approximate solution to calculate the electrostatic field of a thunderstorm cloud can greatly improve the computational accuracy without sacrificing the computational efficiency, which is of great significance for the accurate warning when lightning is approaching.

Keywords: a thunderstorm cloud; electrostatic field; calculation method

MSC: 78-10

check for updates

Citation: Wang, L.; Wan, H.; Chen, Y. Research on the Calculation Method of Electrostatic Field of a Thunderstorm Cloud. *Mathematics* **2022**, *10*, 4132. https://doi.org/10.3390/math10214132

Academic Editor: Yury Shestopalov

Received: 17 September 2022
Accepted: 1 November 2022
Published: 5 November 2022

Publisher's Note: MDPI stays neutral with regard to jurisdictional claims in published maps and institutional affiliations.

Copyright: © 2022 by the authors. Licensee MDPI, Basel, Switzerland. This article is an open access article distributed under the terms and conditions of the Creative Commons Attribution (CC BY) license (https://creativecommons.org/licenses/by/4.0/).

1. Introduction

The strong electric field generated by a thunderstorm cloud in space is an important factor for the initiation and development of lightning, and it also seriously threatens the safety of ground maneuvering targets. Ground maneuvering targets may encounter lightning strikes or induce lightning when passing through areas with a strong electric field, resulting in catastrophic consequences [1,2]. The electrostatic field of a thunderstorm cloud reflects the change of space potential, which is an important basic parameter of the dielectric breakdown model used in the numerical simulation of lightning pilot discharge and the numerical evaluation of lightning protection effectiveness [3,4], which has a great influence on the dimensionality of the lightning pilot discharge graph and the choice of the discharge path. There are many studies on the calculation of the electrostatic field of a thunderstorm cloud [5–7]. Some studies have obtained the structure of a thunderstorm cloud by establishing a system of coupled equations and setting the marginal relations using numerical calculations [8–10], which can obtain the dynamics of a thunderstorm cloud, but it takes a lot of time and cannot obtain the analytical expression. Some studies have obtained a thunderstorm cloud structure using mathematical-physical methods [11,12], which fail to obtain the analytical expression, and the complex arithmetic is also time-consuming. Some studies have used an approximate method to calculate the electrostatic field excited by a thunderstorm cloud and obtained the first-order approximate analytical expression of the electrostatic field of a thunderstorm cloud [7], which shortens the calculation time,

but the error is still relatively large and is not conducive to accurate warning of lightning. The cylindrical charge stack model [13–15] is used to solve the electrostatic field excited by a thunderstorm cloud, based on the theory of electrostatic field in this paper [16], which greatly reduces the error and improves the calculation accuracy without sacrificing the computational efficiency, and lays the foundation for accurate lightning warning.

2. Methods

The cylindrical charge stack model is used to solve the electric field excited by a thunderstorm cloud in a column coordinate system. The radius of the cylinder is a, and the heights of the bottom and top surfaces from the ground are h_1 and h_2 respectively. The thunderstorm cloud charge pile is uniformly charged, and its bulk charge density is ρ. An arbitrary point in the cylindrical charge pile is selected as the charge element, whose coordinate is (r', φ', z'), and R_1, R_2 are the distances between the charge element and the mirror charge element to the observation point. The longitudinal electric field generated by a thunderstorm cloud is:

$$E_z = \frac{\rho}{4\pi\varepsilon_0}\int_{h_1}^{h_2}\int_0^{2\pi}\int_0^a \left(\frac{z'-z}{{R_1}^3}+\frac{z'+z}{{R_2}^3}\right)r'\mathrm{d}r'\mathrm{d}\varphi'\mathrm{d}z'e_z \tag{1}$$

$R_1 = \sqrt{r'^2+r^2-2r'r\cos(\varphi-\varphi')+(2'-z)^2}$, $R_2 = \sqrt{r'^2+r^2-2r'r\cos(\varphi-\varphi')+(z'+z)^2}$, ε_0 is the vacuum permittivity, e_z is the unit vector in the z direction. Equation (1) is the exact solution of the electric field generated by a thunderstorm cloud; the analytical expression cannot be obtained by solving Equation (1), and making an approximation to the product function, let $R_{10} = \sqrt{r'^2+r^2+(z'-z)^2}$, then ${R_1}^{-3}$ is converted into:

$${R_1}^{-3} = {R_{10}}^{-3}\left[1-2r'r\cos(\varphi-\varphi')/{R_{10}}^2\right]^{-3/2} \tag{2}$$

By doing a binomial expansion of the above equation, we can get:

$$\left[1-2r'r\cos(\varphi-\varphi')/{R_{10}}^2\right]^{-3/2} = \sum_{n=0}^{+\infty}\frac{(2n+1)!!}{n!2^n}\left[\frac{2r'r\cos(\varphi-\varphi')}{{R_{10}}^2}\right]^n \tag{3}$$

Substituting Equations (2) and (3) into (1), E_z can be transformed into an integral of infinite polynomials. Since the odd power integral of the cosine function is 0, to ensure the accuracy of the approximation, retains the first two items of Eauation (3), n = 0 and n = 2, then Equation (2) is converted into:

$${R_1}^{-3} \approx {R_{10}}^{-3} + 15{R_{10}}^{-7}r'^2r^2\cos^2(\varphi-\varphi')/2 \tag{4}$$

Let $R_{20} = \sqrt{r'^2+r^2+(z'+z)^2}$, then ${R_2}^{-3}$ is converted into:

$${R_2}^{-3} \approx {R_{20}}^{-3} + 15{R_{20}}^{-7}r'^2r^2\cos^2(\varphi-\varphi')/2 \tag{5}$$

Substituting Equations (4) and (5) into Equation (1), a second-order approximate solution for E_z can be obtained:

$$\begin{aligned} E_z \approx{}& \frac{\rho}{4\pi\varepsilon_0}\int_{h_1}^{h_2}\int_0^{2\pi}\int_0^a\left[\frac{z'-z}{{R_{10}}^3}+\frac{15(z'-z)r'^2r^2\cos^2(\varphi-\varphi')}{2{R_{10}}^7}\right. \\ &\left.+\frac{z'+z}{{R_{20}}^3}+\frac{15(z'+z)r'^2r^2\cos^2(\varphi-\varphi')}{2{R_{20}}^7}\right]r'\mathrm{d}r'\mathrm{d}\varphi'\mathrm{d}z'e_z \end{aligned} \tag{6}$$

Solving the above equation, the approximate expression of the longitudinal electric field generated by a thunderstorm cloud can be obtained as:

$$\begin{aligned} E_z \approx \frac{\rho}{8\varepsilon_0}\Bigg\{ & 4\sqrt{r^2+(h_2-z)^2} - 4\sqrt{r^2+(h_1-z)^2} - 4\sqrt{a^2+r^2+(h_2-z)^2} \\ & +4\sqrt{a^2+r^2+(h_1-z)^2} + 4\sqrt{r^2+(h_2+z)^2} - 4\sqrt{r^2+(h_1+z)^2} \\ & -4\sqrt{a^2+r^2+(h_2+z)^2} + 4\sqrt{a^2+r^2+(h_1+z)^2} \\ & + \frac{2r^2}{\sqrt{r^2+(h_1-z)^2}} - \frac{2r^2}{\sqrt{r^2+(h_2-z)^2}} + \frac{2r^2}{\sqrt{r^2+(h_1+z)^2}} - \frac{2r^2}{\sqrt{r^2+(h_2+z)^2}} \\ & + \frac{3a^2r^2+2r^4+2r^2(h_1-z)^2}{\sqrt{\left[a^2+r^2+(h_1-z)^2\right]^3}} - \frac{3a^2r^2+2r^4+2r^2(h_2-z)^2}{\sqrt{\left[a^2+r^2+(h_2-z)^2\right]^3}} \\ & + \frac{3a^2r^2+2r^4+2r^2(h_1+z)^2}{\sqrt{\left[a^2+r^2+(h_1+z)^2\right]^3}} - \frac{3a^2r^2+2r^4+2r^2(h_2+z)^2}{\sqrt{\left[a^2+r^2+(h_2+z)^2\right]^3}} \Bigg\} e_z \end{aligned} \tag{7}$$

3. Verification

Let the body charge density of the cylindrical charge stack of a thunderstorm cloud be 1 nC/m^3, the radius of the cylinder be 2 km, and the heights of the upper and lower boundaries of the cylinder from the ground be 10 km and 7 km [17]. The exact solution, the first-order approximate solution and the second-order approximate solution are used respectively to calculate the electric field generated by a thunderstorm cloud within the radius of 10 km and the height of 7 km, and the results are shown in Figure 1. It can be found that the error between the second-order approximate solution and exact solution is smaller than the error between the first-order approximate solution and exact solution in the three-dimensional stereogram of Figure 1. The comparison and relative error of the first-order approximate solution, second-order approximate solution and exact solution for r = 0, r = 5 km, h = 0, h = 5 km are shown in Figures 2–5 respectively. It can be seen from the figure that when z = 0 and r = 0–10 km, the maximum error between the first-order approximate solution and the exact solution is about 2.6%, while the error between the second-order approximate solution and the exact solution is always about 0. When z = 5 km and r = 0–10 km, the maximum error between the first-order approximate solution and the exact solution is about 13.2%, while the maximum error between the second-order approximate solution and the exact solution is about 3.1%. When r = 0, the first-order approximate solution and the second-order approximate solution are transformed into the exact solution, so the three lines of electric field coincide completely. When r = 5 km and z = 0–7 km, the error between the first-order approximate solution and the exact solution increases from 0 to 15.1%, while the error between the second-order approximate solution and the exact solution increases from 0 to 4.1% with the increase of height. By comparison, it is found that the error between the second-order approximate solution and the exact solution is significantly smaller than that between the first-order approximate solution and the exact solution.

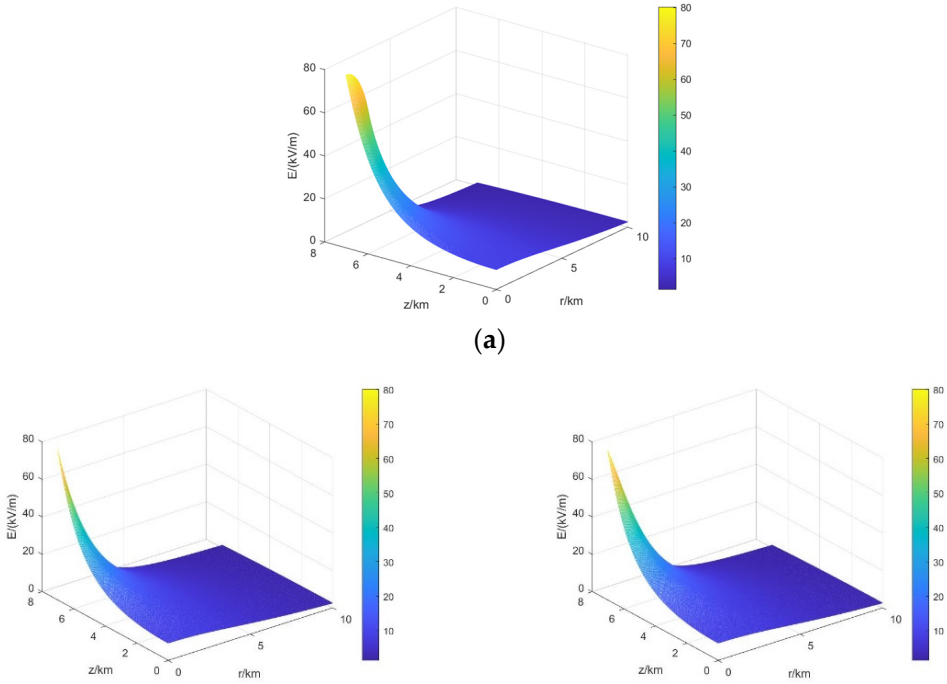


Figure 1. (**a**) Electric field distribution calculated with exact solution. (**b**) Electric field distribution calculated with the first-order approximate solution. (**c**) Electric field distribution calculated with the second-order approximate solution.

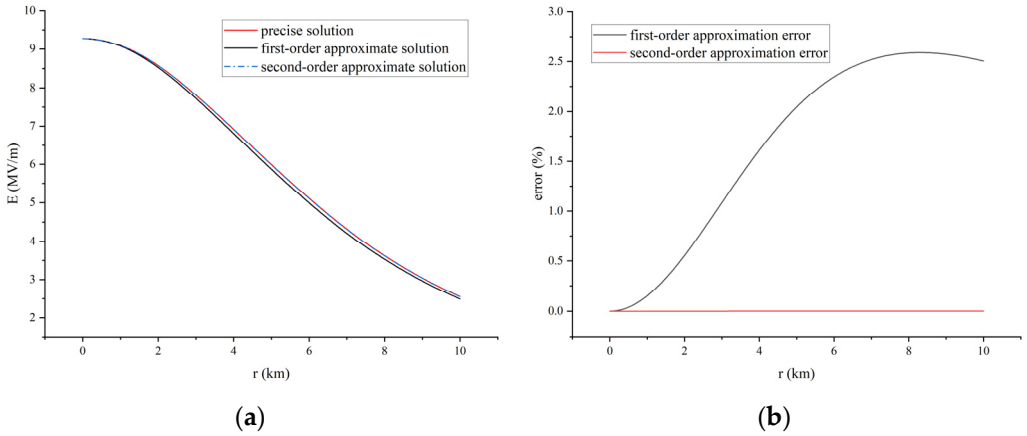


Figure 2. (**a**) Comparison of the first-order approximate solution, second-order approximate solution, and exact solution, while $z = 0$. (**b**) Relative error of first-order approximation and second-order approximation while $z = 0$.

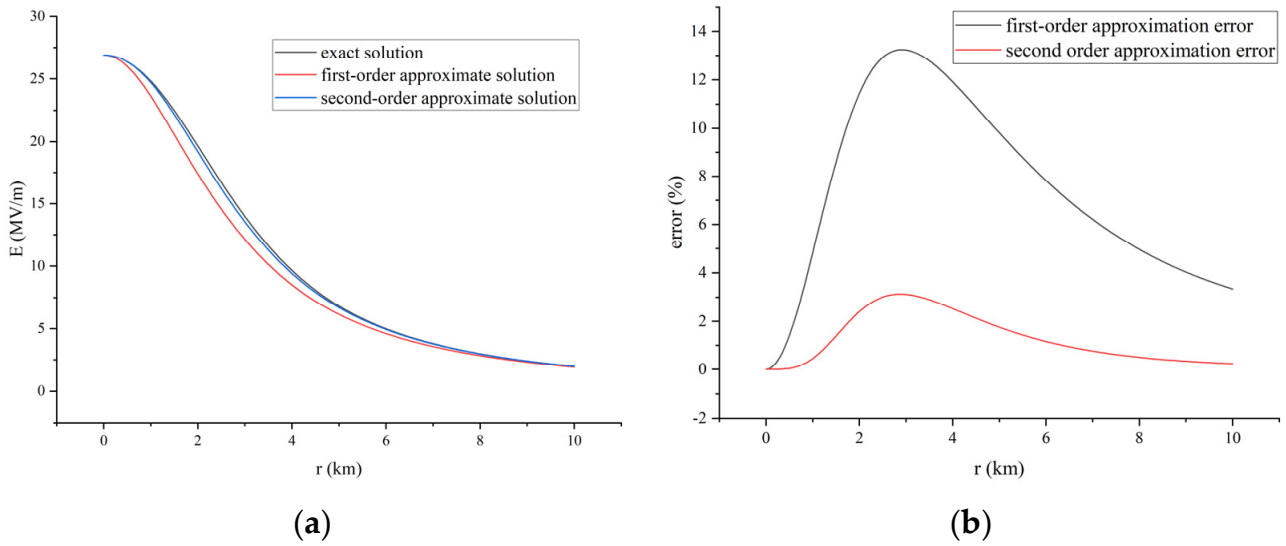


Figure 3. (**a**) Comparison of the first-order approximate solution, second-order approximate solution and exact solution while z = 5 km. (**b**) Relative error of first-order approximation and second-order approximation while z = 5 km.

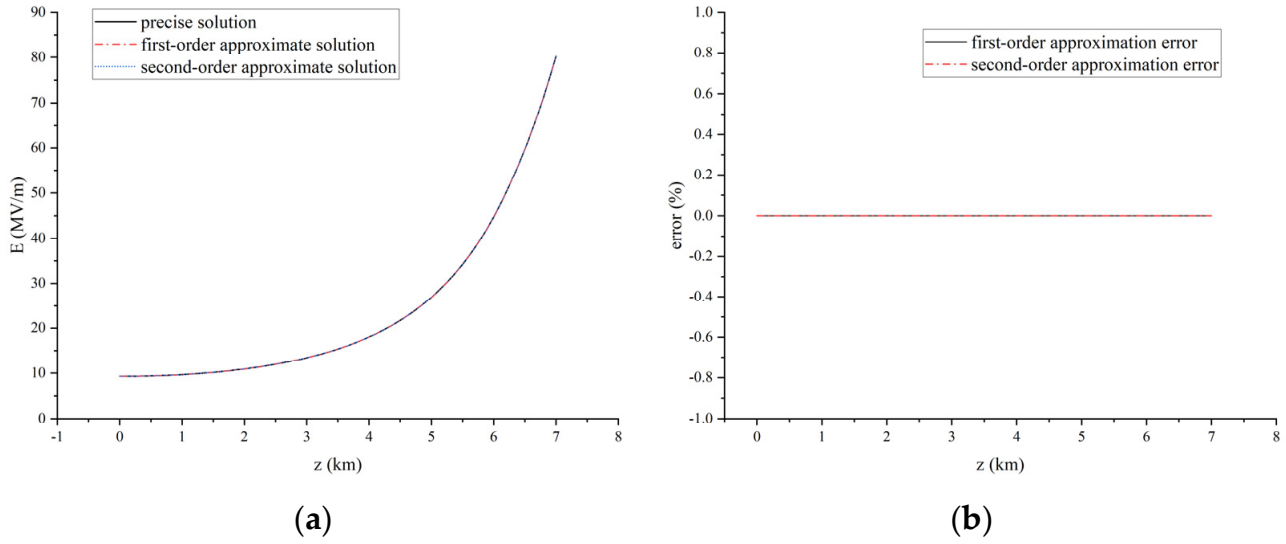
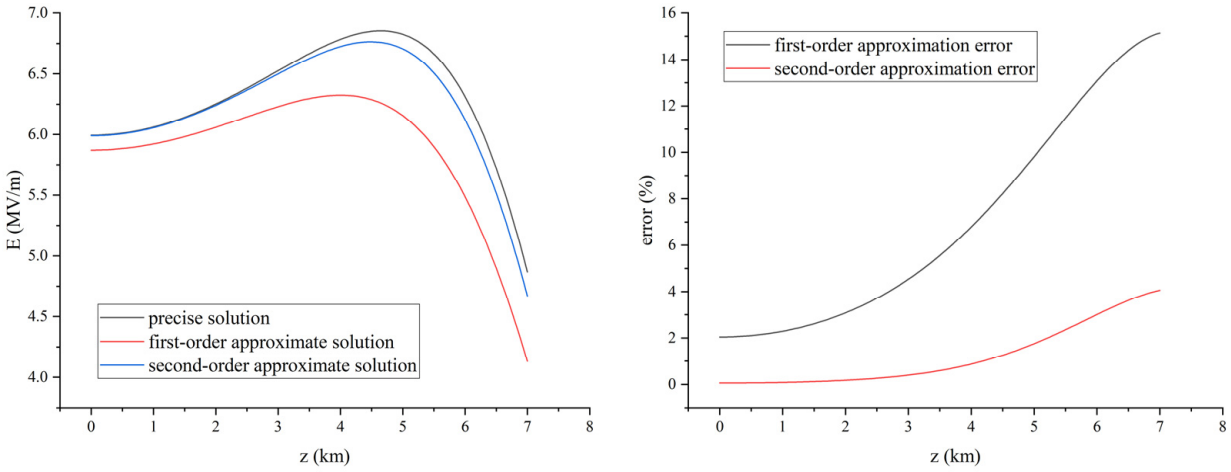


Figure 4. (**a**) Comparison of the first-order approximate solution, second-order approximate solution and exact solution while r = 0. (**b**) Relative error of first-order approximation and second-order approximation while r = 0.



(**a**) (**b**)

Figure 5. (**a**) Comparison of the first-order approximate solution, second-order approximate solution and exact solution while r = 5 km. (**b**) Relative error of first-order approximation and second-order approximation while r = 5 km.

The computation time which is spent on calculating the electrostatic field generated by a thunderstorm cloud are 15,655 s (4.27 h), 0.01 s, and 0.03 s relatively by using the exact solution, the first-order approximate solution, and the second-order approximate solution by the same version of MATLAB (R2021b) on the same configured computer (Inter(R) Core (TM) i5-10210U CPU @ 1.6 GHz 2.11 GHz). It can be seen that compared with the computation time using the exact solution, the computation time using the first-order approximation and the second-order approximation are both greatly reduced, and the computation time is in the same order of magnitude and much less than 1 s. Although the calculation time is slightly longer than that of the first-order approximation solution, the error of the second-order approximation is much smaller than that of the first-order approximation. Therefore, from the perspective of balancing computational accuracy and computational time, the second-order approximate solution should be used in the example calculation of the electrostatic field generated by a thunderstorm cloud.

4. Example Calculation and Analysis

A large number of electric field soundings and charged particle soundings [18–21] within a thunderstorm cloud confirm that a thunderstorm cloud has a simplified tripolar charge structure [22–24] (a positive charge region in the upper part, a negative charge region in the middle part, and a small positive charge region in the lower part). A typical three-level charge structure thunderstorm cloud is selected as the excitation source, and its charge structure and parameters are shown in Figure 6. The electric field distribution and electric field contours of a thunderstorm cloud in the longitudinal section of y = 0, 16 km, 22 km, 30 km and 40 km are shown in Figures 7–11. It can be seen from the figure that the spatial electric field is axially symmetrically distributed at different distances due to the centrosymmetric distribution of the tripole charge pile of the thunderstorm cloud.

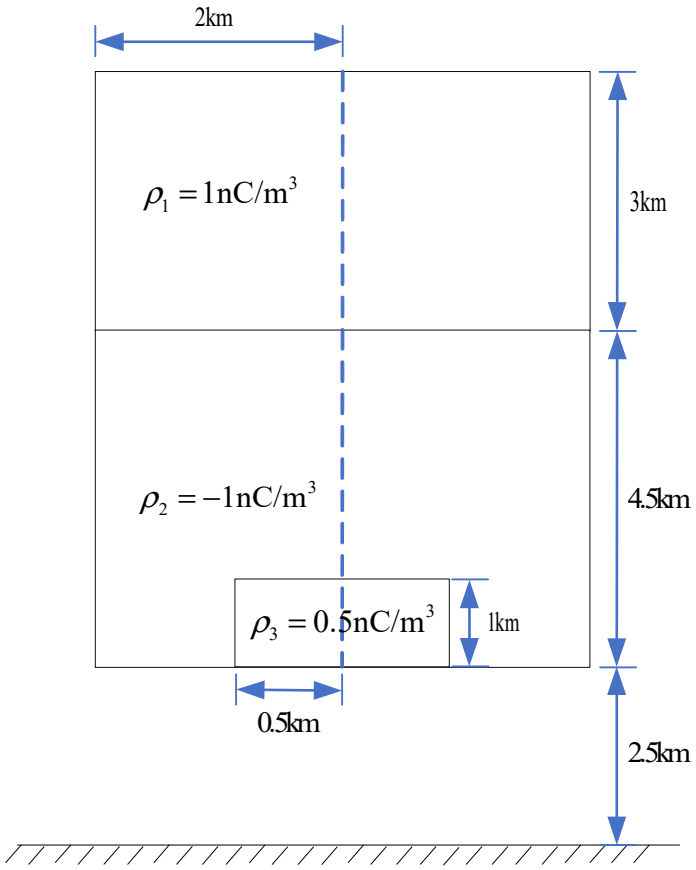
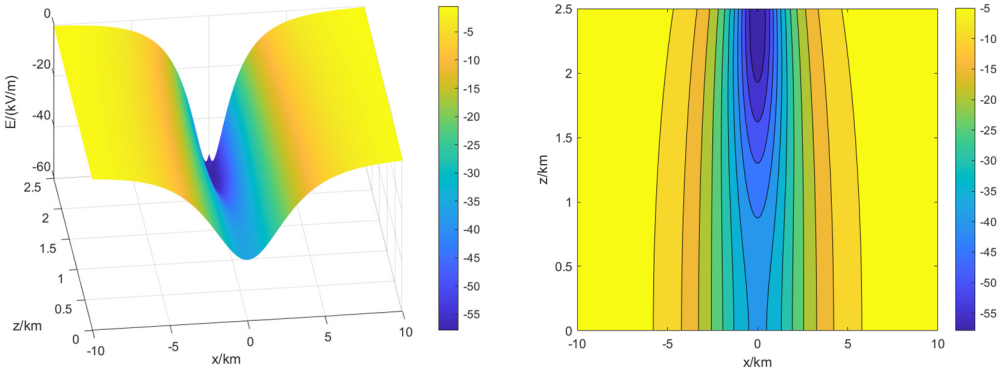
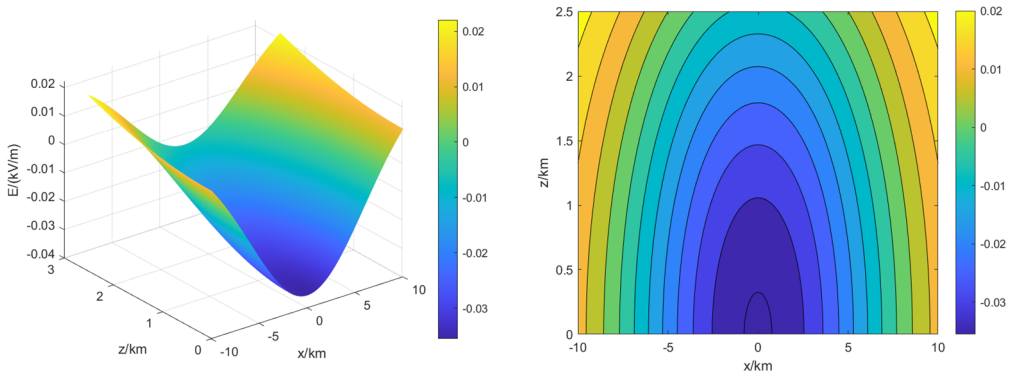


Figure 6. Typical tertiary charge structure of a thunderstorm cloud.



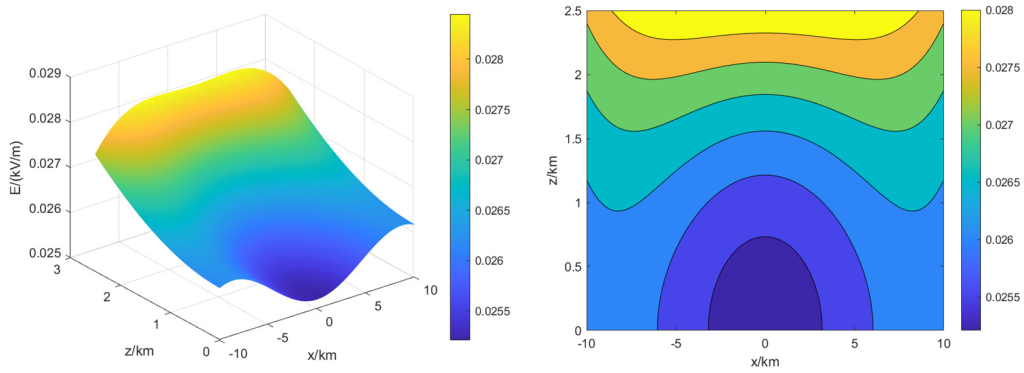
(**a**) (**b**)

Figure 7. (**a**) Electric field distribution on the longitudinal section while $y = 0$. (**b**) Contour of potential distribution on the longitudinal section while $y = 0$.



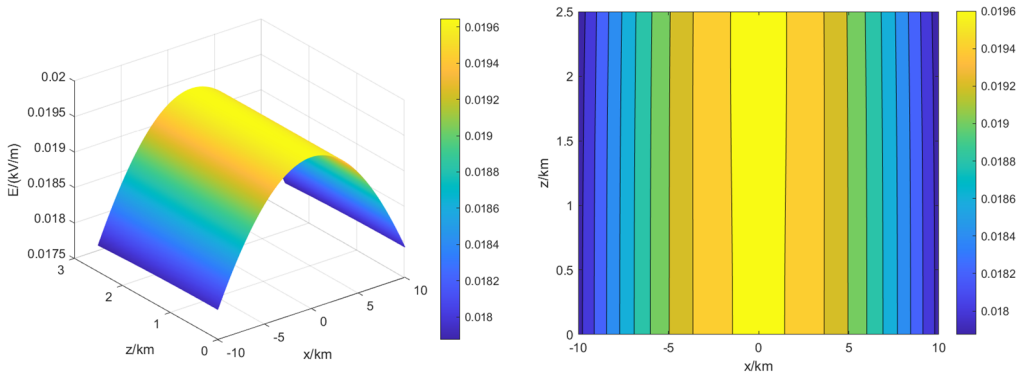
(**a**) (**b**)

Figure 8. (**a**) Electric field distribution on the longitudinal section while y = 16 km. (**b**) Contour of potential distribution on the longitudinal section while y = 16 km.



(**a**) (**b**)

Figure 9. (**a**) Electric field distribution on the longitudinal section while y = 22 km. (**b**) Contour of potential distribution on the longitudinal section while y = 22 km.



(**a**) (**b**)

Figure 10. (**a**) Electric field distribution on the longitudinal section while y = 30 km. (**b**) Contour of potential distribution on the longitudinal section while y = 30 km.

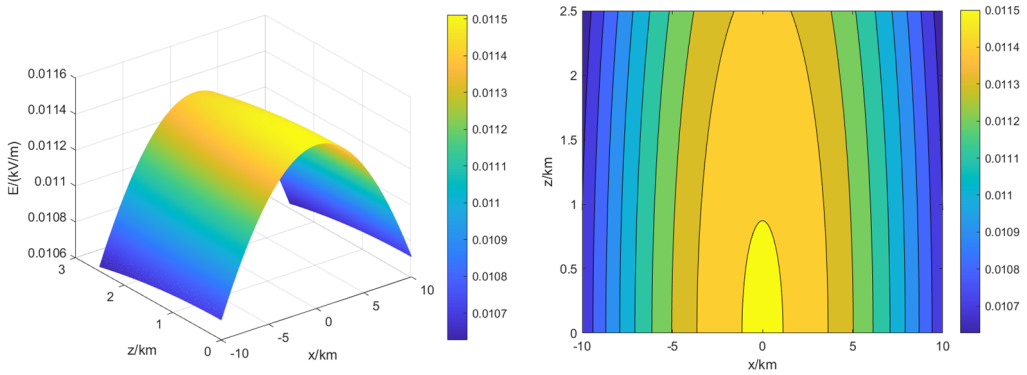


Figure 11. (**a**) Electric field distribution on the longitudinal section while y = 40 km. (**b**) Electric field distribution on the longitudinal section while y = 40.

It can be seen from Figure 7 that a small peak appears in the area close to a thunderstorm cloud on the central axis directly under the thunderstorm cloud, which is caused by the lower positive charge area of the thunderstorm cloud. Due to the small amount of charge in the lower positive charge area, the resulting fluctuations are small. At longer distances, the electric field excited by the lower positively charged region of the thunderstorm cloud is smaller, so no small peaks appear. It can be seen from the above figure that the electric field has a large change rate of distance under the thunderstorm cloud. However, as the distance increases, no matter in the x-direction or the z-direction, the change rate of the electric field to the distance gradually decreases. In other words, the electric field gradient decreases with the increase of the distance. Figure 7 is the electric field distribution and electric field contour on the longitudinal section of y = 0, which is the area directly under the thunderstorm cloud. The electric field is less than 0, which shows that the electric field excited in the negative charge region of a thunderstorm cloud is stronger than that excited in the positive charge region. Figure 8 shows the electric field distribution and electric field contour on the longitudinal section of y = 16 km. It can be seen that at a distance of more than ten kilometers, the electric field has both positive and negative polarities. It shows that the electric field intensity excited by the positive charge region and the negative charge region of a thunderstorm cloud is evenly matched in this region. Figures 9–11 are the electric field distribution and electric field contour on the longitudinal section when y > 20 km. It can be seen that when the distance is more than 20 km, the electric field is always greater than 0 which shows that the electric field excited by the positive charge region of the thunderstorm cloud is stronger than that of the negative charge region in the long-distance region. From the variation trend of the electric field in the above figures, it can be found that the electric field excited by different charge regions of the thunderstorm has different rates of change relative to the distance between the observation point and the thunderstorm cloud. This is the reason for the reversal of the electric field polarity when the distance between the observation point and the thunderstorm cloud changes. The variation trend of the electric field at different distances is observed by comparing the electric field strength at several points. The points with coordinates (0,0), (0,2.5), and (−10,1.25) in the above figure are called point A, point B, and point C. In Figure 7, $E_C > E_A > E_B$. In Figure 8, $E_C > E_B > E_A$. In Figure 9, $E_B > E_C > E_A$. In Figure 10, $E_B > E_A > E_C$. In Figure 11, $E_A > E_B > E_C$. It can be found that the electric field excited by different charge regions has different magnitudes of increase or decrease with the change of distance. Point A, point B, and point C are three typical location points in the calculation area, and through the comparison of the above figures, it is found that the farther the observation point is from the thunderstorm cloud, the closer the electric field of point A, point B, and point C is. It can be inferred that at infinity, the electric field of point A, point B, and point C are equal, and are all 0, which conforms to the law of electrostatic field, which is consistent with the actual observation data of an electric field excited by a thunderstorm cloud [15].

5. Conclusions

In this paper, the electrostatic field excited by a thunderstorm cloud in space is derived, and the second-order approximate solution of the electrostatic field is obtained by approximation. The calculation of the electrostatic field for different distances and heights reveals that the error between the second-order approximation and the exact solution is significantly smaller than the error between the first-order approximation and the exact solution. The computation time of the electrostatic fields excited by a thunderstorm cloud is of the same order of magnitude and much less than 1 s when the same version of MATLAB is used on the same configuration of computers. By comparison, it is found that the difference in computation time between the second-order approximation and the first-order approximation is small but the error is greatly reduced, which greatly improves the computational accuracy without sacrificing computational efficiency. The electric field excited by a thunderstorm cloud with a typical tertiary charge structure is calculated by using the second-order approximation solution, and the calculated results match with the actual observations, which verifies the correctness of the derivation and the validity of the approximation.

Author Contributions: Writing—original draft preparation, L.W.; writing—review and editing, H.W. and Y.C. All authors have read and agreed to the published version of the manuscript.

Funding: This research was funded by National Natural Science Foundation of China and Key laboratory Foundation, grant number 51707203 and 6142205200401. The APC was funded by Key laboratory Foundation.

Data Availability Statement: Not applicable.

Conflicts of Interest: The authors declare that they have no conflict of interest.

References

1. Zeng, R.; Zhou, X.; Wang, Z.Z.; Zhuang, C.J.; Yu, Z.Q.; He, J.L. Progress and Frontier Review of International Lightning Protection Research. *High Volt.* **2015**, *41*, 2–10. [CrossRef]
2. Zhao, Z.K.; Qie, X.S.; Zhang, G.S.; Zhang, T.L.; Zhang, T.; Guo, F.X.; Dou, Z.Q. Electric field detector in thunderstorm cloud and preliminary experimental results. *Plateau Meteorol.* **2008**, *04*, 881–887.
3. Chen, W.J.; He, H.X.; He, J.J.; Zhao, X.G.; Yu, H.; Shi, W.D.; He, T.Y. Three-dimensional simulation model of lightning pilot development of transmission line. *Chin. J. Electr. Eng.* **2014**, *34*, 6601–6612. [CrossRef]
4. Wan, H.J.; Wei, G.H.; Chen, Q.; Chen, Y.Z. 3D Numerical Simulation and Application of Lightning Pilot Discharge. *High Volt.* **2013**, *39*, 430–436.
5. Guimaraes, M.; Vale, M.H.; Visacro, S. Electric Field During Upward Connecting Leader Initiation in Negative Cloud-to-Ground Lightning Measured at a 50-m Distance. *IEEE Trans. Electromagn. Compat.* **2018**, *60*, 2061–2064. [CrossRef]
6. Liu, S.J.; Zhou, X.G. Precise Mathematical Solution of the Global Near-Earth Steady-State Atmospheric Electric Field Considering Thunderstorm Activity. *Acta Geophys.* **2009**, *52*, 1451–1456.
7. Wang, L.; Wan, H.; Chen, Y. Approximate Calculation and Feature Analysis of Electric Field in Space by Thunderclouds. *Int. J. Antennas Propag.* **2021**. [CrossRef]
8. Tan, Y.B.; Tao, S.C.; Zhu, B.Y.; Ma, M.; Lv, W.T. Numerical simulation of the influence of cloud lightning discharge on the distribution of electric charge and potential in the cloud. *Acta Geophys.* **2007**, *04*, 1053–1065.
9. Tzur, I.; Levin, Z. Ions and precipitation charging in warm and cold clouds as simulated in one-dimensional time-dependent models. *Atmos. Sci.* **1981**, *38*, 2444–2461. [CrossRef]
10. Takahasi, T. Numerical simulation of warm cloud electricity. *Atmos. Sci.* **1974**, *31*, 2160–2181. [CrossRef]
11. Chen, Q.; Wei, G.H. Study of thundercloud charge model. *Adv. Geophys.* **2010**, *25*, 1617–1622.
12. Chen, Q.; Wei, G.H. Quantum inversion of thundercloud charging model. *Acta Geophys.* **2010**, *53*, 2237–2243.
13. Francesco, L. *Electromagnetic Compatibility in Power Systems*; China Machine Press: Beijing, China, 2008; pp. 30–33.
14. Amoruso, V.; Lattarulo, F. Thundercloud pre-stroke electrostatic modeling. *Electrost.* **2002**, *56*, 255–276. [CrossRef]
15. Williams, E. Charge structure and geographical variation of thunderclouds. In *The Lightning Flash*; Cooray, V., Ed.; IET: London, UK, 2003.
16. Guo, S.H. *Electrodynamics*; Beijing Higher Education Press: Beijing, China, 2008; Volume 3, p. 4.
17. Qie, X.S.; Zhang, Q.L.; Yuan, T.; Zhang, T.L. *Lightning Physics*; Science Press: Beijing, China, 2013.
18. Marshall, T.C.; Rust, W.D. Electric field soundings through thunderstorms. *J. Geophys. Res. Atmos.* **1991**, *96*, 22297–22306. [CrossRef]

19. Marshall, T.C.; Rison, W.; Rust, W.D.; Stolzenburg, M.; Willett, J.C.; Winn, W.P. Rocket and balloon observations of electric field in two thunderstorms. *J. Geophys. Res. Atmos.* **1995**, *100*, 20815–20828. [CrossRef]
20. Zhang, H.; Qie, X.; Liu, M.; Jiang, R.; Lu, G.; Liu, R.; Liu, D.; Chen, Z.; Sun, Z.; Li, Z.; et al. Observation of charge structure within primary thunderstorm clouds based on bimetallic sphere 3D electric field sounding instrument. *J. Geophys.* **2021**, *64*, 1155–1166.
21. Zhang, T.; Yu, H.; Wang, J.; Zhang, M.; Zhou, F.; Chen, J. Ground flash activity of a thunderstorm in Qinghai area and electric field sounding observation within the cloud. *J. Geophys.* **2019**, *62*, 1591–1602.
22. Krehbiel, P.R. The electrical structure of thunderstorms. In *The Earth's Electrical Environment*; Krider, E.P., Roble, R.G., Eds.; National Academy Press: Washington, DC, USA, 1998; pp. 90–113.
23. Williams, E.R. The tripole structure of thunderstorms. *J. Geophys. Res.* **1989**, *94*, 13151–13167. [CrossRef]
24. Li, J.; Yu, Y.; Li, W.; Li, Y. Numerical simulation study on the effects of different non-induced initiation and induced initiation parameterization schemes on the charge structure of primary thunderstorm clouds in eastern Qinghai. *J. Geophys.* **2019**, *62*, 2366–2381.